Correlation of the electronic and atomic structure at passivated *n*-InP(100) surfaces

© M.V. Lebedev[1], T.V. Lvova[1], A.N. Smirnov[1], V.Yu. Davydov[1], A.V. Koroleva[2], E.V. Zhizhin[2], S.V. Lebedev[2]

[1] Ioffe Institute,
194021 St. Petersburg, Russia
[2] St. Petersburg State University,
199034 St. Petersburg, Russia

E-mail: mleb@triat.ioffe.ru

Received March 2, 2022
Revised March 25, 2022
Accepted March 25, 2022

Photoluminescence, Raman spectroscopy and X-ray photoelectron spectroscopy are used to study electronic and atomic structure of *n*-InP(100) surfaces treated with different sulfide solutions. It is shown that the sulfide treatment causes removal of the native oxide layer from the semiconductor surface and formation of the passivating layer consisting of In−S chemical bonds with the structure dependent on the solution composition and atomic arrangement at the initial surface of the semiconductor. This is accompanied by an increase in photoluminescence intensity and narrowing of the surface depletion layer. Atomic structure of the passivating layer determines the total dipole that modifies the depth distribution of the bands potentials and thus the surface electronic structure.

Keywords: surface modification, sulfur passivation, Raman spectroscopy, photoluminescence, X-ray photoelectron spectroscopy.

DOI: 10.21883/SC.2022.07.54648.11

1. Introduction

Indium phosphide (InP) is one of the most important III−V semiconductor materials actively used in modern electronic and optoelectronic devices [1–4], as well as in nanostructures [5–8].

The characteristics of nanostructures are determined in a great extent by the properties of surfaces and interfaces. Surfaces of III−V semiconductors are characterized by high density of surface states in the band gap, which leads to the high velocity of non-radiative surface recombination. Therefore, surface passivation is often necessary to reduce electronic and optical losses in nanostructures, as well as to stabilize chemically their surface [9]. One of the most widely used methods for passivating the surface of III−V semiconductors is treatment with sulfide-containing solutions or gases. In particular, sulfide passivation has been used to modify the electronic properties of InP-based nanowires [10], as well as InP/insulator [11–13] interfaces.

Sulfide passivation leads to the removal of the native oxide layer from the semiconductor surface and to the formation of a passivating coating on it, which prevents surface oxidation and modifies the spectrum of surface states. In addition, it was found that the composition of the sulfide solution could have a significant effect on the efficiency of the electronic passivation of the surface [14]. As a rule, electronic passivation of the surface manifests itself as an increase in the intensity of edge photoluminescence (PL), which indicates a decrease in the surface recombination velocity [13,15,16]. Nevertheless, the reasons for the decrease in the non-radiative recombination at the *n*-InP(100) surface are still not clear, since the band bending at the *n*-InP(100) surface remains essentially unchanged after sulfide passivation [16–18]. In this regard, it is necessary to analyze the effect of passivation in various solutions on the atomic and electronic structures of the InP(100) surface.

In this paper, the electronic and atomic structures of *n*-InP(100) surfaces treated with aqueous or alcoholic sulfide solutions are studied by photoluminescence (PL), Raman scattering (RS) spectroscopy, and X-ray photoelectron spectroscopy (XPS) in order to find the relationship between the electronic passivation efficiency and the atomic structure of the passivated surface.

2. Experimental procedure

Samples were cleaved from *n*-InP(100) wafers with the doping levels of $6 \cdot 10^{17}$ and $2 \cdot 10^{18}\,\mathrm{cm}^{-3}$. The wafer with the doping level of $6 \cdot 10^{17}\,\mathrm{cm}^{-3}$ was cut from a crystal grown by the Czochralski method, while the wafer with the doping level of $2 \cdot 10^{18}\,\mathrm{cm}^{-3}$ was the epitaxial layer of corresponding concentration with the thickness of 2 microns grown on an *n*-InP(100) substrate. After preliminary washing in toluene and acetone [18], the samples were treated for various times with one of the ammonium sulfide $[(NH_4)_2S]$ solutions, in which concentration or solvent was varied. As solutions, either the standard aqueous solution of ammonium sulfide ($(NH_4)_2S$ (40−48 wt% in H_2O)), Merck-Sigma-Aldrich), hereinafter denoted as

Treatment (solution, treatment time)	n-InP(100), $6 \cdot 10^{17}$ cm^{-3} [18]			n-InP(100), $2 \cdot 10^{18}$ cm^{-3}		
	Intensity PL, rel. units	V_B, eV	δ nm	Intensity PL, rel. units	V_B, eV	δ, nm
Initial (non-treated)	1	0.17	15.6	1	0.21	7.2
$(NH_4)_2S_{aq}$ (4%), 10 min	4.2	0.27	8.1	–	–	–
$(NH_4)_2S_{aq}$ (44%), 10 min	5.75	0.17	10.5	–	–	–
$(NH_4)_2S + 2PA$, 10 min	7.9	0.17	9.0	0.75	0.36	6.1
$(NH_4)_2S + 2PA$, 1 min	10.9	0.17	6.2	–	–	–
$(NH_4)_2S + 2PA$, 2 min	–	–	–	1.25	0.36	6.1

standard aqueous $(NH_4)_2S$ solution with concentration of $\sim 44\%$, or ammonium sulfide solutions prepared from the standard one by diluting with water or 2-propanol to the concentration of $\sim 4\%$. After sulfide treatment, the samples were rinsed with water (or 2-propanol for alcoholic-solution-treated samples) and dried in air.

Micro-PL and micro-RS were carried out in air at room temperature using T64000 spectrometer (Horiba JobinYvon, Lille, France) with confocal microscope. To excite the spectra, the line of a He–Cd laser (Plasma, Inc., Russia) with the wavelength $\lambda = 442$ nm (2.81 eV) was used. When measuring the PL spectra, the laser beam was focused into the spot with diameter of $\sim 1\,\mu$m. During PL measurements, the radiation density did not exceed 50 W/cm^2. The micro-RS spectra were measured at radiation density of ~ 5.5 kW/cm^2 at the same point of the sample as the micro-PL spectra.

XPS studies were carried out on an Escalab 250Xi photoelectron spectrometer using an AlK_α source with a photon energy of 1486.6 eV. The binding energy was referred to Fermi level. The binding energy scale was calibrated by measuring the Au $4f_{7/2}$ (84.0 eV) and Cu $2p_{3/2}$ (932.7 eV) core level spectra using a special calibration sample. The residual vacuum pressure in the analysis chamber was better than $1 \cdot 10^{-9}$ mbar.

3. Results and discussion

After sulfide treatment in any of the considered solutions, the PL intensity of n-InP(100) with a doping level of $6 \cdot 10^{17}$ cm^{-3} increased significantly [18] (see Table), indicating the electronic passivation of the surface. The highest efficiency of electronic passivation was achieved after surface treatment of n-InP(100) in $(NH_4)_2S + 2PA$ alcoholic solution. As in the case of the surface treatment with 1 M aqueous Na_2S solution [16], the greatest increase in the PL intensity was achieved at a short-term (~ 1 min) surface treatment.

Surface treatment of the n-InP(100) with the doping level of $2 \cdot 10^{18}$ cm^{-3} with alcoholic solution did not lead to a significant increase in the PL intensity of n-InP(100) (Fig. 1 and Table). As in the case of a less doped semiconductor [18], the PL spectrum of the initial untreated n-InP(100) represents an asymmetric peak with a maximum at energy of about 1.37 eV. This value corresponds approximately to the energy difference between the valence band edge and the Fermi level in the semiconductor bulk [19]. Besides, a small feature is observed in the spectrum at energy corresponding to the band gap of indium phosphide at room temperature (1.344 eV [20]).

After treatment of the n-InP(100) surface with the doping level of $2 \cdot 10^{18}$ cm^{-3} in alcoholic $(NH_4)_2S$ solution for 2 min, the PL intensity increased by $\sim 25\%$ (Fig. 1 and Table). Longer treatment for 10 min led to the degradation of electronic passivation so that the PL intensity decreased to a level of $\sim 25\%$ lower than the value characteristic of the initial untreated n-InP(100) surface (Fig. 1 and Table).

RS spectra of n-InP(100) with different doping levels measured before and after surface treatment with

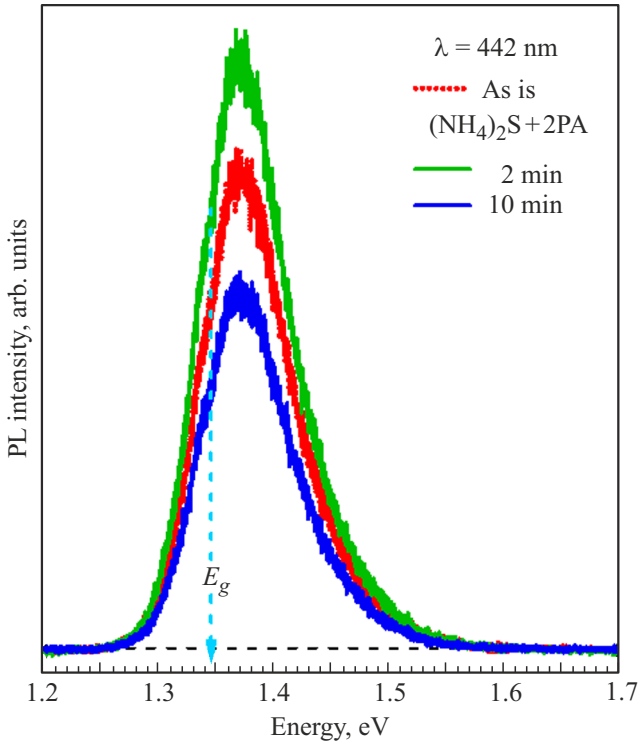

Figure 1. PL spectra of n-InP(100) with the doping level of $2 \cdot 10^{18}$ cm^{-3} measured before and after treatment with $(NH_4)_2S$+2PA solution for 2 and 10 min. (A color version of the figure is provided in the online version of the paper).

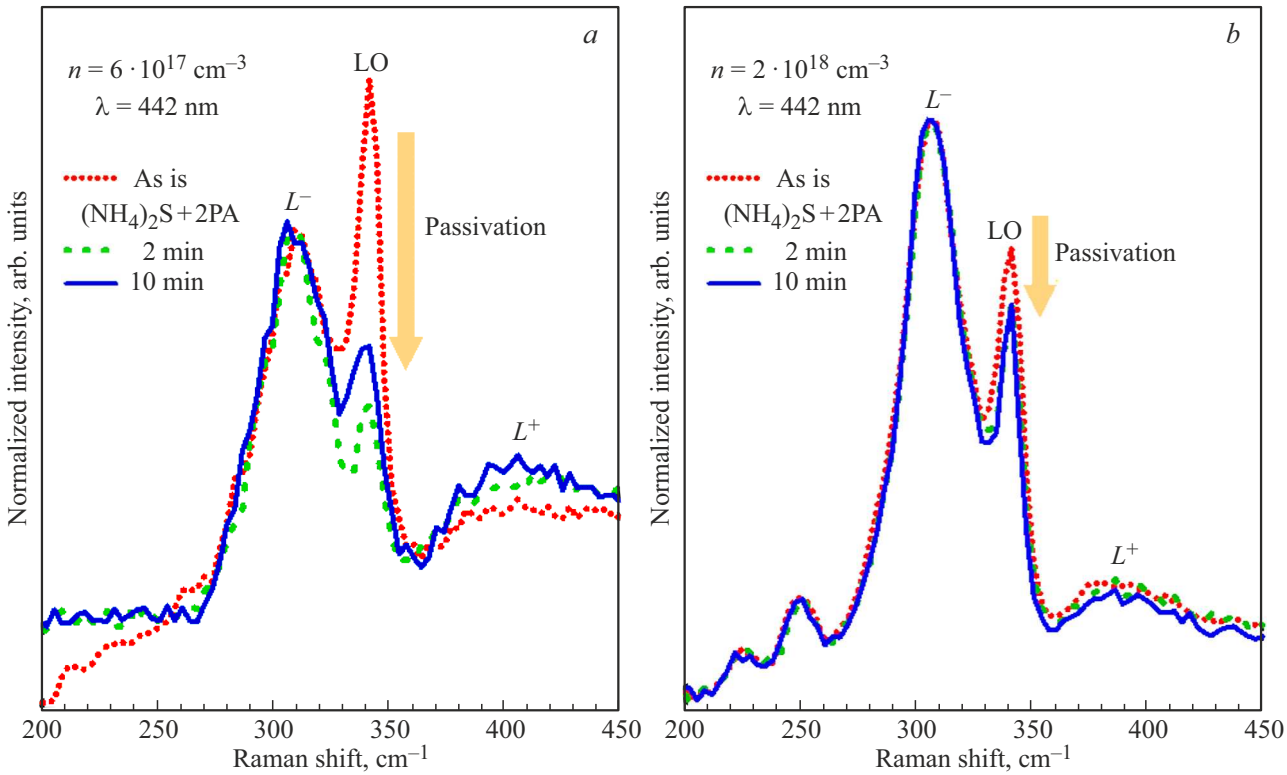

Figure 2. RS spectra of *n*-InP(100) with doping levels of $6 \cdot 10^{17}$ (*a*) and $2 \cdot 10^{18}$ cm^{-3} (*b*) measured before and after treatment with $(NH_4)_2S + 2PA$ solution for 1–2 and 10 min.

$(NH_4)_2S + 2PA$ solution for different times are shown in Fig. 2. The RS spectra of the initial samples have a shape typical for *n*-doped InP(100) [21]. In particular, the spectra exhibit the LO peak (~ 341 cm^{-1}) stemming from scattering by longitudinal optical phonons in the near-surface depletion layer, as well as L^- (306 cm^{-1}) and the L^+ bands associated with scattering by phonons and plasmons in the semiconductor bulk. The position of the L^+ band maximum corresponds to the doping level of the used sample [22].

After sulfide treatment of *n*-InP(100) with the doping level of $6 \cdot 10^{17}$ cm^{-3} the ratio of LO and L^- peak intensities decreased significantly [18], which indicates a narrowing of the near-surface depletion layer [23]. The greatest decrease in the ratio of intensities (more than by a factor of 3) was observed when *n*-InP(100) was treated with the $(NH_4)_2S + 2PA$ solution for 1 min (Fig. 2, *a*). Longer treatment with the alcoholic $(NH_4)_2S$ solution or treatment with aqueous $(NH_4)_2S$ solutions led to a somewhat smaller decrease in the ratio of the intensities of the LO and L^- peaks (by a factor of 1.5–2.0) [18].

Effect of sulfide treatment of *n*-InP(100) with the doping level of $2 \cdot 10^{18}$ cm^{-3} on the ratio of LO and L^- peak intensities was significantly smaller (Fig. 2, *b*). Thus, after treatment with $(NH_4)_2S + 2PA$ solution for 2 or 10 min, the ratio of the intensities of LO and L^- peaks decreased by $\sim 17\%$ (Fig. 2, *b*).

Thus, treatment of the *n*-InP(100) with sulfide solutions leads to electronic passivation of its surface. To elucidate the mechanism of electronic passivation, the chemical composition and electronic structure of the passivated *n*-InP(100) surfaces were studied by XPS. In general, treatment with sulfide solutions leads to the removal of the native oxide layer from the InP(100) surface and the formation of a passivating coating consisting mainly of indium sulfides [16–18].

Typical spectra of P 2*p* and In 4*d* core levels, measured before and after sulfide treatment of the *n*-InP(100) surface, are shown in Fig. 3. As was shown earlier [16–18], the initial *n*-InP(100) surface before sulfide treatment is covered with a native oxide layer consisting of indium phosphates and oxides. Treatment with any of the sulfide solutions considered leads to almost identical changes in the P 2*p* and In 4*d* core level spectra. For example, after surface treatment with a standard $(NH_4)_2S$ aqueous solution for 10 min, the layer of indium phosphates is completely removed from the *n*-InP(100) surface, and instead of the component associated with indium oxides In_xO_y, a component related to indium sulfides appears in the In 4*d* core level spectrum (Fig. 3). Surface treatment with any other of the solutions considered leads to similar changes in the P 2*p* and In 4*d* core level spectra [18].

The positions of the P–In and In–P bulk components in the fitting of the P 2*p* and In 4*d* core-level spectra were used

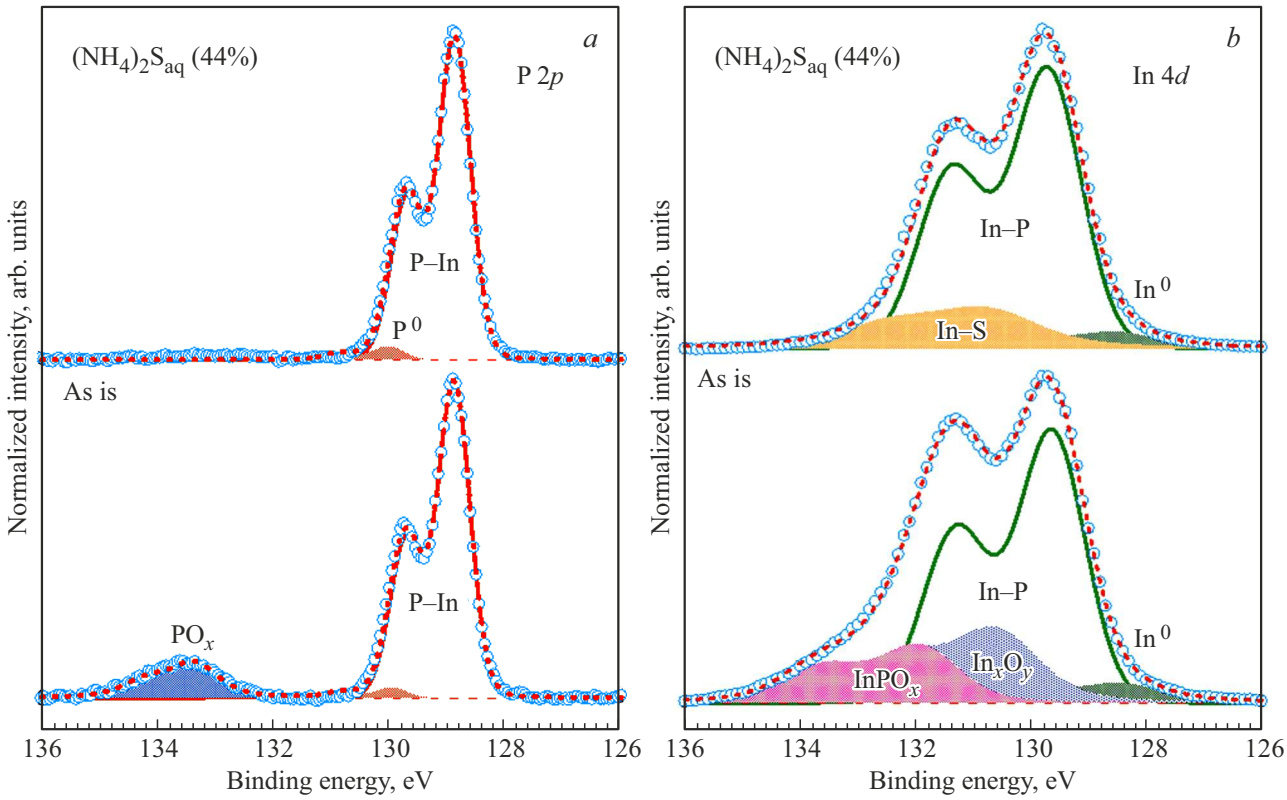

Figure 3. Fitting of the spectra of P 2*p* (*a*) and In 4*d* (*b*) core levels measured before and after treatment of the *n*-InP(100) surface with standard aqueous $(NH_4)_2S$ solution for 10 min.

to determine the band bending values for the *n*-InP(100) surfaces before and after treatment with various sulfide solutions. For InP, the binding energies of the P−In($2p_{3/2}$) and In−P($4d_{5/2}$) bulk components relative to the edge of the valence band (E_{VBM}) are 127.74 eV [24,25] and 16.65 eV [26], respectively. The values of the band bending estimated in this way (the position of the conduction band minimum (E_{CBM}) relative to the Fermi level on the surface), averaged over the data for the P−In($2p_{3/2}$) and In−P($4d_{5/2}$) bulk components are presented in the Table.

Thus, treatment of the *n*-InP(100) surface with sulfide solutions leads to a modification of the surface electronic properties, which manifests itself as an increase in the PL intensity and change in the shape of the RS spectra, indicating decrease in the near-surface depletion layer. In this case, the value of the near-surface band bending remained unchanged or even increased (see Table). Based on the obtained values of the near-surface band bending V_B, the doping level n, and taking into account the transition layer width $\delta_t \sim 4.4$ nm [27], it is possible to estimate the width of the near-surface depletion layer δ_0 in the initial untreated InP by the formula

$$\delta_0 = \sqrt{\frac{\varepsilon_0 V_B}{2\pi n e^2}} - \delta_t, \qquad (1)$$

where ε_0 is the static dielectric constant of InP ($\varepsilon_0 = 12.5$), and e is the electron charge. The values of the near-surface depletion layer width δ_0 calculated by formula (1) in initial InP samples with the doping levels of $6 \cdot 10^{17}$ and $2 \cdot 10^{18}$ cm^{-3} were 15.6 and 7.2 nm, respectively (see Table). The width of the near-surface depleted layer in the InP samples treated with sulfide solutions was calculated from the ratios of the peak intensities I(LO)/I(L^-) in the RS spectra, similarly to the works [18,27]. The obtained values are presented in the Table.

After treating the *n*-InP(100) surface with sulfide solutions, the P 2*p* and In 4*d* core level spectra (Fig. 3) look very similar, regardless the solution used and the treatment time [18], while the electronic properties of such surfaces differ significantly (see Table). In this case, despite a significant decrease in the width of the near-surface depletion layer, the band bending V_B remains unchanged, or even increases in some cases. Thus, the width of the near-surface depletion layer in the passivated *n*-InP(100) is no longer described by formula (1). This indicates that the near-surface band bending in passivated *n*-InP(100) is determined not only by the density of surface states, but also by the potential of surface dipoles [18].

To elucidate the reasons for the change in the potential of the surface dipole upon treatment of *n*-InP(100) with various sulfide solutions, we analyzed the S 2*p* core level spectra measured on passivated surfaces. The spectra of the S 2*p* core level can be decomposed into three components with binding energies approximately of

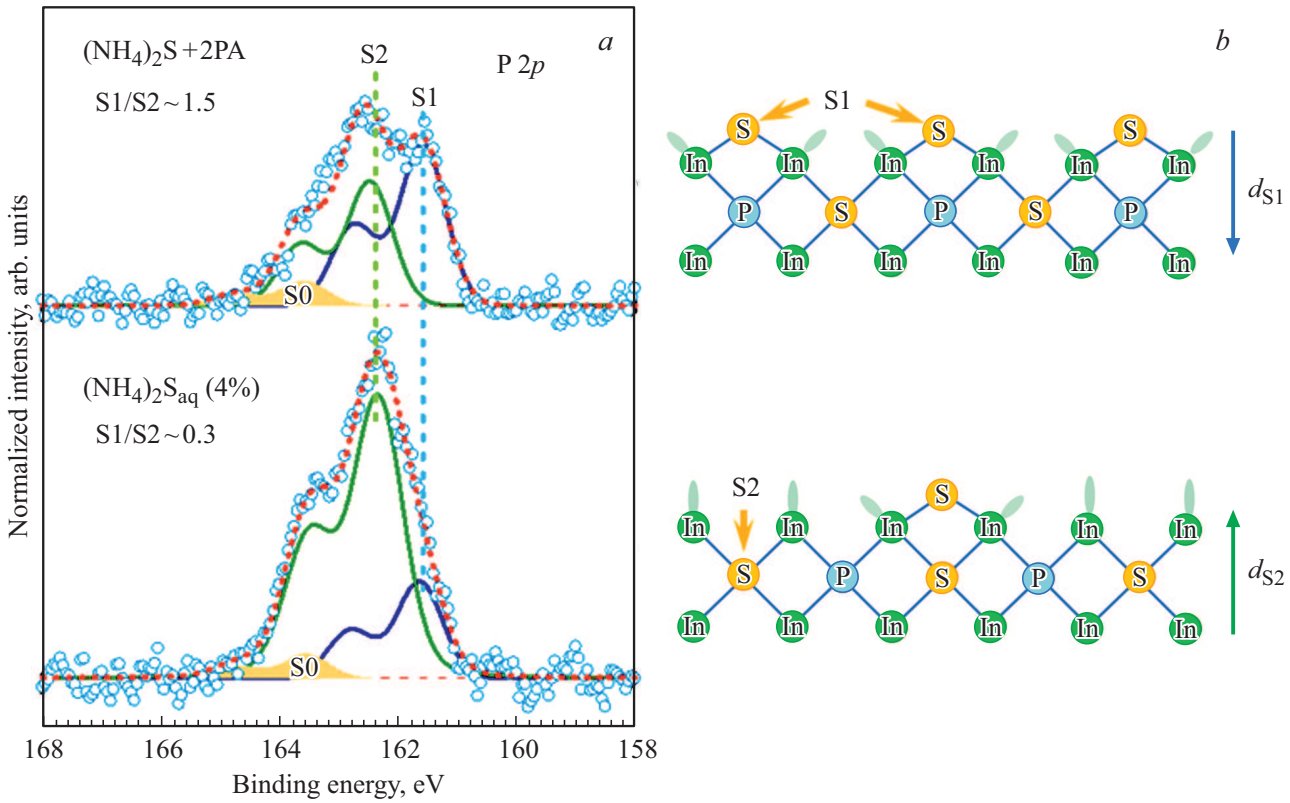

Figure 4. *a* — fitting of typical S 2*p* core level spectra [18] measured after treatment of *n*-InP(100) ($n = 6 \cdot 10^{17}$ cm^{-3}) surface with indicated sulfide solutions. *b* — schematic representation for the atomic structure of these passivated surfaces.

161.4 (S1), 162.15 (S2) and 163.2 eV (S0) (Fig. 4, *a*). The S1 component can be assigned to sulfur atoms in the In−S−In bridge bonds, and the S2 component is related to sulfur atoms occupying phosphorus vacancies in the near-surface monolayer of semiconductor [13] (Fig. 4, *b*). The S0 component is associated with excess sulfur in the form of polysulfide clusters on the semiconductor surface. It should be noted that the ratio of the intensities of S1 and S2 components differed after treatment of the *n*-InP(100) surface with various sulfide solutions (Fig. 4, *a*). Moreover, comparison of the S1/S2 ratio values with the corresponding values of the PL intensity and the width of the near-surface depletion layer (Fig. 5) shows that for the passivated *n*-InP(100) with the doping level of $6 \cdot 10^{17}$ cm^{-3}, the PL intensity increases with an increase in the S1/S2 ratio. The increase in PL intensity indicates an increase in the efficiency of surface electronic passivation. In almost all cases, the width of the near-surface depletion layer decreases in accordance with an increase in the PL intensity (Fig. 5). The only exception is the treatment of the surface with a dilute aqueous $(NH_4)_2S$ solution with a concentration of 4% for 10 min, after which the PL intensity did not increase as much as it should be expected from the observed narrowing of the near-surface depletion layer (Fig. 5). After such treatment, the component S2 dominated in the S 2*p* core level spectrum (Fig. 4, *a*), however, in this case, simultaneously with the narrowing of the near-surface depletion layer, an increase in the near-surface band bending V_B was observed (see Table) indicating Fermi level re-pinning in the band gap.

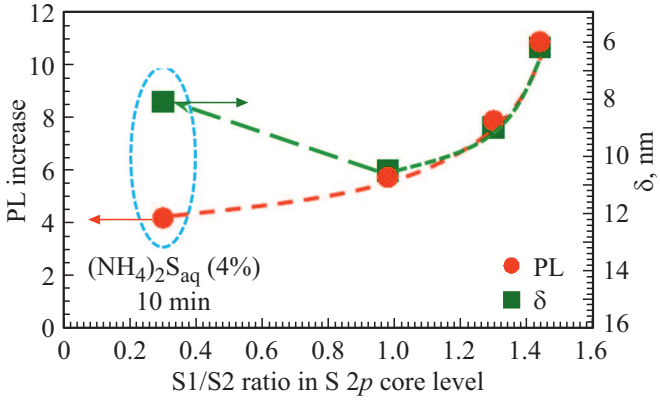

Figure 5. Correlation between the increase in PL intensity, the width of the space charge layer δ, and the ratio of the intensities of the S1 and S2 components in the fitting of the S 2*p* core level spectra of the *n*-InP(100) surface with the doping level of $6 \cdot 10^{17}$ cm^{-3}, passivated with various sulfide solutions. For the original (untreated) *n*-InP(100) surface, the increase in PL intensity is 1, and the value $\delta = 15.6$ nm. The experimental data was used from [18].

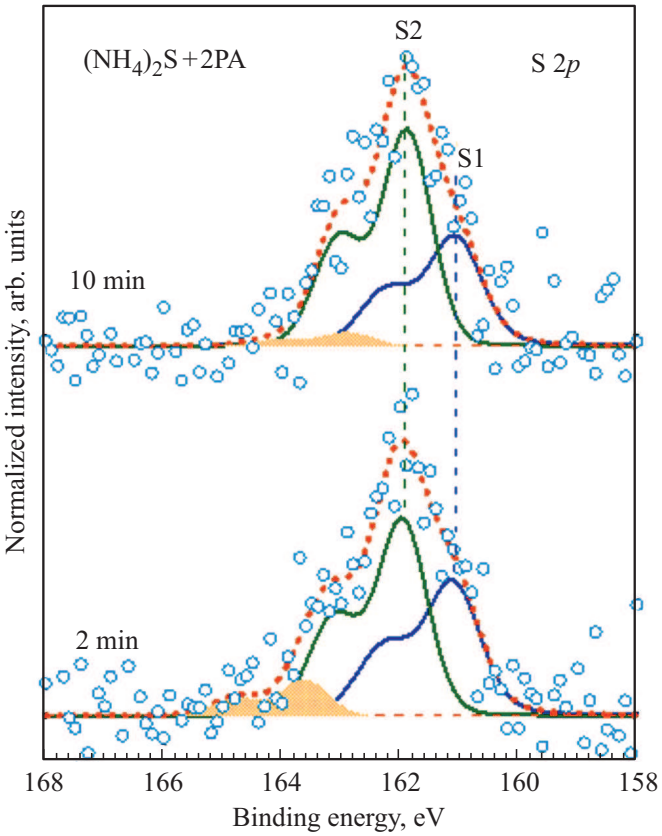

Figure 6. Fitting of the S $2p$ core level spectra measured after treatment of the n-InP(100) surface ($n = 2 \cdot 10^{18}\,\mathrm{cm}^{-3}$) with $(NH_4)_2S + 2PA$ solution for various times.

On the other hand, treatment of the n-InP(100) surface with the doping level of $2 \cdot 10^{18}\,\mathrm{cm}^{-3}$ with alcoholic $(NH_4)_2S + 2PA$ solution also resulted in the increase in the near-surface band bending V_B along with narrowing of the near-surface depletion layer (see Table). At the same time, in the fitting of the S $2p$ core level spectra the S2 component prevailed (Fig. 6) so that the S1/S2 ratios were 0.77 and 0.57 for treatment times of 2 and 10 min, respectively.

The In−S−In bridge bonds (state S1, Fig. 4, b), as well as the In−S−In bonds, in which sulfur atoms occupy phosphorus vacancies (state S2, Fig. 4, b) have a dipole moment due to the difference in the electronegativity of sulfur and indium atoms. The dipole moment d_{S1} due to the state S1 and the dipole moment d_{S2} due to the state S2 are directed oppositely (Fig. 4, b). In general, the magnitude of these dipole moments can differ, for example, due to the difference between interatomic distances [28,29] and the charges of sulfur atoms in the S1 and S2 states.

Thus, the total surface dipole due to the In−S bonds formed after sulfide treatment should depend on the S1/S2 components ratio in the fitting of the S $2p$ core level spectra (Fig. 4, a). If most of the sulfur atoms are in the S1 state (Fig. 4, b), then the direction of the total surface dipole will correspond to d_{S1}. According to theoretical calculations [29], such a sulfide coating structure should be the most stable. In the case of n-InP(100) with a doping level of $6 \cdot 10^{17}\,\mathrm{cm}^{-3}$, this atomic structure provides the most efficient electronic passivation of the surface (Fig. 5). And vice versa, if the state S2 predominates in the fitting of the S $2p$ spectrum, then the surface dipole will have opposite direction (corresponding to d_{S2}). As a result, the Fermi level may be re-pinned on the surface of the passivated n-InP(100), since the direction of the dipole field (Fig. 4, b) coincides with the direction of the field in the near-surface depleted layer. Namely, the direction and magnitude of the total surface dipole will depend on the atomic structure of the sulfide layer, which, in turn, will be determined by the characteristics of the chemical processes occurring during sulfide passivation. Change in the near-surface dipole will modify the band potential distribution on the semiconductor surface and, therefore, the electronic structure of its surface.

It should be noted that the ratio of the number of sulfur atoms in the S1 and S2 states in the sulfide coating on the InP(100) surface can be dependent not only on the sulfide solution composition. Indeed, when the n-InP(100) surface with the doping level of $6 \cdot 10^{17}\,\mathrm{cm}^{-3}$ was treated with $(NH_4)_2S + 2PA$ solution, the sulfide coating characterized by the ratio S1/S2 ~ 1.5 is formed (Fig. 4, a). On the other hand, after treatment of the n-InP(100) surface with the doping level of $2 \cdot 10^{18}\,\mathrm{cm}^{-3}$ with the same solution, the S1/S2 ratio in the formed sulfide coating was significantly less than 1 (Fig. 6). This result can be explained by the influence of the atomic structure of the initial semiconductor surface on the chemical processes of sulphidizing. In particular, the In/P atomic concentrations ratio on the initial n-InP(100) surface with the doping level of $6 \cdot 10^{17}\,\mathrm{cm}^{-3}$ was ~ 1.7, and after treatment with any of the considered solutions, this ratio decreased to 1.6 [18]. On the n-InP(100) surface with a doping level of $2 \cdot 10^{18}\,\mathrm{cm}^{-3}$ the In/P ratio was 1.15, and after sulphidizing in $(NH_4)_2S + 2PA$ solution it increased to ~ 1.35.

Thus, when studying the electronic passivation of the n-InP(100) surface by sulfide solutions, it is necessary to consider the whole variety of chemical and electronic processes at the semiconductor/solution interface, taking into account the initial atomic and electronic structure of the semiconductor surface, as well as the composition of the solution.

4. Conclusion

Using photoluminescence, Raman scattering spectroscopy, and X-ray photoelectron spectroscopy, the electronic and atomic structures of n-InP(100) surfaces treated with various sulfide solutions were studied in order to establish the relationship between the efficiency of electronic passivation and the atomic structure of the passivated surface. It is shown that the treatment of the n-InP(100) surface with sulfide solutions leads to an increase in the PL intensity, accompanied by narrowing of the near-surface

depleted layer of the semiconductor. After treatment with sulfide solutions, the oxide layer is removed from the semiconductor surface and a passivating coating is formed. This passivating coating consists of two types of In−S bonds, such as In−S−In bridge bonds and bonds in which the sulfur atoms occupy phosphorus vacancies in the near-surface monolayer. The fraction of sulfur atoms in bonds of one type or another will determine the total dipole moment, which in turn will determine the spatial distribution of the band potential and, therefore, the electronic structure of the surface. Electronic passivation is the most effective when In−S−In bridge bonds predominate. When most of sulfur atoms occupy phosphorus vacancies, the Fermi level is re-pinned and the near-surface band bending increases, which leads to a decrease in the electronic passivation efficiency.

Funding

The research was supported in part by the Russian Foundation for Basic Research (RFBR) (Project No. 20-03-00523). XPS studies were supported financially by the Saint Petersburg State University (project No. 93021679).

Acknowledgments

The work was performed using the equipment of the Resource Center „Physical methods of surface investigations“ of the Scientific Park of St. Petersburg State University.

Conflict of interest

The authors declare that they have no conflicts of interest.

References

[1] J.A. del Alamo. Nature, **479**, 317 (2011).
[2] M. Smit, K. Williams, J. van der Tol. APL Photonics, **4**, 050901 (2019).
[3] A.G. Muñoz, C. Heine, M. Lublow, H.W. Klemm, N. Szabó, T. Hannappel, H.-J. Lewerenz. ECS J. Solid State Sci. Technol., **2**, Q51 (2013).
[4] Q. Lin, D. Sarkar, Y. Lin, M. Yeung, L. Blankemeier, J. Hazra, W. Wang, S. Niu, J. Ravichandran, Z. Fan, R. Kapadia. ACS Nano, **11**, 5113 (2017).
[5] X. Duan, Y. Huang, Y. Cui, J. Wang, C.M. Lieber. Nature, **409**, 66 (2001).
[6] F. Zafar, A. Iqbal. Proc. Royal Soc. A, **472**, 20150804 (2016).
[7] Z. Li, I. Yang, L. Li, Q. Gao, J. S. Chong, Z. Li, M.N. Lockrey, H.H. Tan, C. Jagadish, L.Fu. Progr. Nat. Sci. Mater., **28**, 178 (2018).
[8] Z. Wu, P. Liu, W. Zhang, K. Wang, X.W. Sun. ACS Energy Lett., **5**, 1095 (2020).
[9] P.R. Narangan, J.D. Butson, H.H. Tan, C. Jagadish, S. Karuturi. Nano Lett., **21**, 6967(2021).
[10] N. Tajik, C.M. Haapamaki, R.R. LaPierre. Nanotechnology, **23**, 315703 (2012).
[11] C.-F. Yen, M.-K. Lee. J. Vac. Sci. Technol. B, **30**, 052201 (2012).
[12] H.-K. Kang, Y.-S. Kang, M. Baik, K.-S. Jeong, D.-K. Kim, J.-D. Song, M.-H. Cho. J. Phys. Chem. C, **122**, 7226 (2018).
[13] D.H. van Dorp, L. Nyns, D. Cuypers, T. Ivanov, S. Brizzi, M. Tallarida, C. Fleischmann, P. Hönicke, M. Müller, O. Richard, D. Schmeißer, S. De Gendt, D.H.C. Lin, C. Adelmann. ACS Appl. Electron. Mater., **1**, 2190 (2019).
[14] M.V. Lebedev. Semiconductors, **54**, 699 (2020).
[15] S. Tian, Z. Wei, Y. Li, H. Zhao, X. Fang, J. Tang, D. Fang, L. Sun, G. Liu, B. Yao, X. Ma. Mater. Sci. Semicond. Process., **17**, 33 (2014).
[16] M.V. Lebedev, Yu.M. Serov, T.V. Lvova, R. Endo, T. Masuda, I.V. Sedova. Appl. Surf. Sci., **533**, 147484 (2020).
[17] M.V. Lebedev, Yu.M. Serov, T.V. Lvova, I.V. Sedova, R. Endo, T. Masuda. Semiconductors, **54**, 1843 (2020).
[18] M.V. Lebedev, T.V. Lvova, A.N. Smirnov, V.Yu. Davydov, A.V. Koroleva, E.V. Zhizhin, S.V. Lebedev. J. Mater. Chem. C, **10**, 2163 (2022).
[19] R.M. Sieg, S.A. Ringel. J. Appl. Phys., **80**, 448 (1996).
[20] L. Pavesi, F. Piazza, A. Rudra, J.F. Carlin, M. Ilegems. Phys. Rev. B, **44**, 9052 (1991).
[21] L. Artús, R. Cuscó, J. Ibáñez, N. Blanco, G. González-Díaz. Phys. Rev. B, **60**, 5456 (1999).
[22] B.B. Boudart, B. Prévot, C. Schwab. Appl. Surf. Sci., **50**, 295 (1991).
[23] V.N. Bessolov, M.V. Lebedev, D.R.T. Zahn. J. Appl. Phys., **82**, 2640 (1997).
[24] J.R. Waldrop, E.A. Kraut, C.W. Farley, R. W. Grant. J. Appl. Phys., **69**, 372 (1991).
[25] Y. Ishikawa, T. Fukui, H. Hasegawa. J. Vac. Sci. Technol. B, **15**, 1163 (1997).
[26] A.B. Preobrajenski, S. Schömann, R.K. Gebhardt, T. Chassé. J. Vac. Sci. Technol. B, **18**, 1973 (2000).
[27] A. Pinczuk, A. A. Ballman, R. E. Nahory, M. A. Pollack, J.M. Worlock. J. Vac. Sci. Technol., **16**, 1168 (1979).
[28] O.L. Warren, G.W. Anderson, M.C. Hanf, K. Griffiths, P.R. Norton. Phys. Rev. B, **52**, 2959 (1995).
[29] A.C. Ferraz, G.P. Srivastava. Appl. Surf. Sci., **142**, 23 (1999).